RSC Applied Polymers

ROYAL SOCIETY OF CHEMISTRY

PAPER

View Article Online
View Journal | View Issue

Cite this: *RSC Appl. Polym.*, 2024, **2**, 456

Enhancing microplastic capture efficiencies with adhesive coatings on stainless-steel filters†

Malavika Ramkumar, [a] Woojung Ji,[a] Henry E. Thurber, [b] Madeline E. Clough, [a] Sarena Chirdon[a] and Anne J. McNeil *[a,b]

Received 15th December 2023,
Accepted 28th February 2024

DOI: 10.1039/d3lp00282a

rsc.li/rscapplpolym

Microplastics have been found in our food, water, and air, raising concerns about their potential health impacts. While environmental remediation may be intractable, we should prioritize minimizing our exposure. In this context, an adhesive-coated stainless-steel filter was developed herein to remove microplastics from water.

Introduction

Microplastics are typically formed *via* the erosion and abrasion of larger plastic materials. Examples include tire wear on roads[1] and washing of synthetic textiles.[2] As rain,[3] wind,[4] and rivers[5] transport and disperse these microplastics throughout the environment, their remediation becomes challenging. Instead, efforts should focus on preventing more microplastics from entering the environment. At the same time, we should also focus on minimizing human exposure to what is already out there. It is within this latter context that microplastic contamination in drinking water (tap and bottled) has gained attention. In 2018, California became the first state to mandate testing of microplastic levels in drinking water and will ultimately set maximum allowable limits.[6,7] As a result, technologies that can meet these standards are urgently needed.[8–10]

To date, researchers have evaluated the microplastic removal efficiencies of existing technologies within drinking water treatment plants.[11–14] Most plants include purification *via* coagulation/sedimentation and filtration through sand or activated carbon followed by disinfection. Overall, these studies have shown that *large* microplastics are effectively removed, but *small* microplastics (10–45 μm (ref. 11) or 10–20 μm (ref. 12)) are more likely to pass through. In addition, Andrews and co-workers discovered that airborne microplastics (which are <10 μm) can be introduced during water treatment due to atmospheric deposition, negating the impacts of earlier removal steps.[11] As such, additional technologies will likely be needed to effectively remove these smaller microplastics from drinking water.

Filtration is a common approach for water purification, and often employed in homes and businesses as an add-on water treatment step. Most filters rely on mechanical filtration, wherein particles become physically trapped on the filter (Scheme 1). The size of particle that is trapped depends on the mesh size, which corresponds to the size of the openings (in microns). Smaller mesh sizes trap more particles, but there is a trade-off between the size of the opening and the water flow rate. In an extreme example, ultrafiltration has small mesh sizes (0.01–0.1 μm), which can effectively capture the smaller microplastics,[15] but the flow rate is too slow unless high pressures are used.

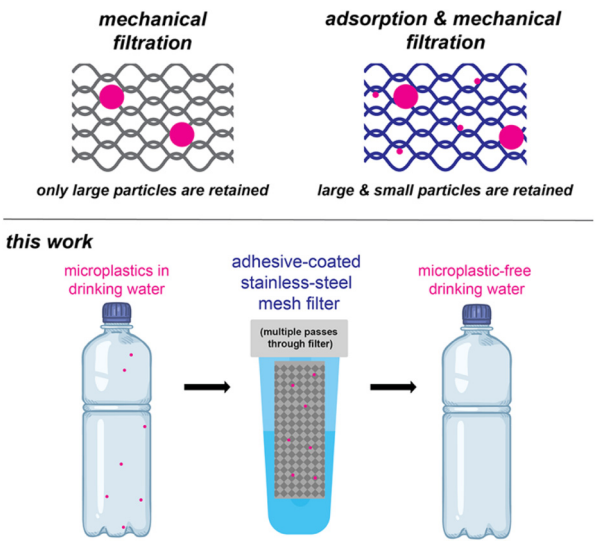

Scheme 1 Filtering mechanisms (top) and an adhesive-coated stainless-steel filter for removing microplastics from drinking water (bottom).

[a]*Department of Chemistry, University of Michigan, 930 North University Avenue, Ann Arbor, MI 48109-1055, USA. E-mail: ajmcneil@umich.edu*
[b]*Macromolecular Science and Engineering Program, University of Michigan, 2300 Hayward Street, Ann Arbor, MI 48109-2800, USA*

† Electronic supplementary information (ESI) available. See DOI: https://doi.org/10.1039/d3lp00282a

Rather than decrease the mesh size, an alternative option is to coat mechanical filters with materials that can leverage adsorption processes.[16–19] With adsorption, the particles are retained due to non-covalent interactions. For example, Guo and co-workers coated wood sawdust with ionically crosslinked polyphenol, which enhanced capture of both nano- and microplastics.[20] Similarly, Quan and co-workers coated a porous loofah sponge with natural waxes to create a superhydrophobic coating that absorbed oil containing hydrophobic polystyrene (PS) microplastics from a water mixture.[21] In another example, Qu and co-workers coated an aluminosilicate-based synthetic porous material with polydimethylsiloxane, creating a hydrophobic surface that captured polyethylene (PE), polypropylene (PP), and poly(vinyl chloride) (PVC) microplastics from water (99% removal at a concentration 1 g L^{-1}).[22] Similarly, we previously reported coating zirconium silicate beads with a pressure-sensitive adhesive (poly(2-ethylhexyl acrylate), P_{EH}) to capture microplastics from water, including PS, poly(ethylene terephthalate), nylon-12, and rubber.[23] Pressure sensitive adhesives[24] are appealing materials for coatings because they can quickly conform to and wet materials such as microplastics. Although high removal efficiencies (>99%) of PS microplastics were observed within 5 min, the concentrations were high (1 g L^{-1}; approx. 10^8 PS microplastics per L) relative to what is most often observed in drinking water (average <10 microplastics per L, range 0–1000 microplastics per L).[25] To achieve high removal efficiencies at lower concentrations, we explore herein the role of filter material and architecture, adhesive chemical structure, as well as microplastic size and identity. This work culminates in quantitative removal of microplastics from water using an adhesive-coated stainless-steel mesh filter under realistic microplastic concentrations.

Results and discussion

Adhesives are advantageous as coating materials because they can be deposited with simple techniques (*e.g.*, dip-coating, solvent-casting, or spray-coating), making this approach both versatile and low-cost. Additionally, some pressure-sensitive adhesives (*i.e.*, poly(alkyl acrylate)s) can be synthesized from waste diapers as the feedstock, which we previously showed results in 22% fewer emissions than the analogous route from petroleum feedstocks.[26] As such, using these diaper-based adhesives as filter coatings herein reduces both macro- and microplastic pollution.

One challenge with pressure-sensitive adhesive coatings is that they have low glass transition temperatures (<0 °C), meaning that the chains are mobile at room temperature. Consequently, the adhesives can, over time, move across and off the coated substrate, leading to uneven coatings and shedding. We observed this undesirable phenomenon in our previous system[23] with P_{EH}-coated zirconium silicate beads (Fig. 1A and Fig. S26 and S27†). Clumps of adhesive formed between the beads after stirring for 18 h in a microplastics/water/ethanol mixture. To overcome this challenge, we evaluated herein both alternative adhesives and substrates to identify an adhesive/substrate combination that exhibits a more stable coating and maintains fast removal efficiencies.

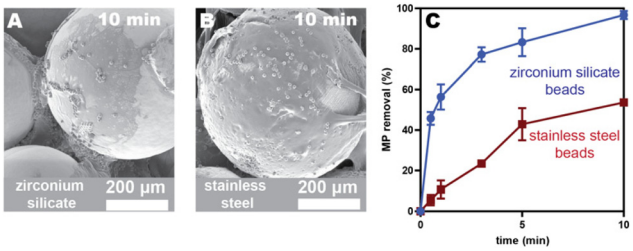

Fig. 1 SEM images of P_{EH} spray-coated zirconium silicate beads (A) and stainless-steel beads (B) after 10 min of a capture experiment. (C) Plot of microplastic removal efficiencies (percent removed relative to a control) *versus* time (min), as quantified by flow cytometry. All capture experiments were performed in 80/20 water/ethanol solutions containing 500 mg L^{-1} of PS microplastics (10 μm diameter).

Identifying the optimal substrate material

Spherical beads were chosen as the initial architecture because they can be packed into columns for large-scale, high-flow-rate filtration. To improve surface wetting and stability, stainless-steel (SS) beads were selected due to its high surface energy relative to the adhesive.[27] Additional advantages include its low cost and high corrosion resistance. To compare the wetting and stability, the original adhesive (P_{EH}, M_w = 735 kDa) was spray-coated onto both SS and zirconium silicate beads. Spray-coating enables the adhesive solution to be aerosolized and propelled forward as a fine mist. Once deposited, the solvent quickly evaporates, producing a more even coating than the original solvent-casting methods.[23] The coated SS beads were stirred in an aqueous suspension of microplastics for 18 h to compare to the zirconium silicate beads. The SS coatings appeared more stable *via* scanning electron microscopy (SEM), though some evidence of adhesive migration was still visible (Fig. S26 and S27†). Nevertheless, stainless steel offered a significant improvement in adhesive retention over the zirconium silicate substrates.

To compare the relative capture efficiencies of SS and zirconium silicate beads, both adhesive-coated beads were agitated in vials with polystyrene microplastics (10 μm, 500 mg L^{-1}) suspended in an 80/20 water/ethanol mixture to prevent microplastic clumping. Aliquots were taken at different time intervals for analysis using flow cytometry.[23] Removal efficiencies were calculated by comparing the microplastic counts in the sample relative to the control (Table S3†). As evident in Fig. 1C, after 10 min the P_{EH}-coated SS beads exhibited lower microplastic removal efficiencies (54 ± 2%) compared to the zirconium silicate beads (97 ± 2%). While disappointing, we realized that the large adhesive clumps that form between the zirconium silicate beads (due to adhesive migration) is likely responsible for this more efficient capture. Because adhesive shedding would be problematic in a drinking water appli-

cation, we moved forward with stainless steel as the substrate for all future studies.

Identifying the optimal substrate architecture

We next evaluated stainless-steel mesh filters[28] because the web-like architecture should facilitate more contact with microplastics, and the higher surface area might reduce adhesive migration. This architecture was inspired by similar filters marketed for microplastics capture in washing machine effluent. The average width of the openings in our mesh are approximately 3 and 1 mm, much larger than any microplastic examined herein (Table S1†). To efficiently coat the mesh filter with adhesive, we unrolled the material and spray-coated both sides with a 1 wt% solution of P_{EH} in THF. We also dip-coated the mesh with the same solution for comparison. After coating, the mesh was packed into a small vial and a vertical shaker was used to pass the water through the mesh multiple times. Aliquots were removed *via* a syringe fitted with a wide-gauge needle and analyzed *via* flow cytometry. The P_{EH}-coated SS mesh showed faster capture rates (97 ± 1% at 10 min; black data in Fig. 2C) than the SS beads (maroon data in Fig. 1C) at 500 mg L^{-1} concentrations. Interestingly, the uncoated mesh (as purchased) removed 50 ± 3% at 10 min (pink data in Fig. 2C), demonstrating that there is some nonspecific adsorption to the stainless steel and that the adhesive enhances microplastics capture. In both cases, the driving force for microplastics capture is likely to minimize unfavorable interactions with water (*i.e.*, hydrophobic interactions).[29] In the case of the adhesive-coated substrate, there is likely an additional benefit from favorable dispersive interactions between the microplastics and adhesive.[23,30] Notably, the dip-coated substrates exhibited more even and higher coverage than spray-coating (by SEM), and as a result, gave faster removal efficiencies (Fig. S46†). Consequently, all further studies were done with dip-coated materials.

Identifying the optimal adhesive structure

We next explored whether alternative poly(alkyl acrylate)-based adhesives would exhibit stronger adhesion to SS than the original P_{EH}, which could result in better and more stable coatings. Specifically, we measured the force of adhesion using a probe-tack protocol for a series of poly(alkyl acrylate)s from an "acrylate polymer kit" purchased from Scientific Polymer Products (Fig. 3, top). Of these nine adhesives, poly(isobutyl acrylate) (P_{iB}) and our original adhesive (P_{EH}) emerged as the leading materials based on their higher forces of adhesion to SS (Fig. 3A). Nevertheless, these commercial adhesives had a relatively low molar mass (M_w of 45–141 kDa), and we had previously shown that low molar mass adhesives perform better at short times but are more likely to shed adhesive (possibly *via* dissolution) over longer times.[23,31] As a result, we synthesized higher molar mass derivatives of both P_{iB} (M_w = 233 kDa) and P_{EH} (M_w = 735 kDa) for further evaluation. Probe-tack testing of these higher molar mass polymers with stainless steel revealed similar forces of adhesion for both P_{iB} and P_{EH} (Fig. 3B). As such, we surmised that either adhesive would work for this application. We ultimately chose P_{EH} over P_{iB} for all further studies because it is accessible *via* the synthetic route from waste plastics.[26]

Impact of microplastic size and identity

To understand the impact of microplastic identity, the capture of PE and PS microplastics of the same size (10 μm) and concentration (500 mg L^{-1}) were compared. The PS microplastics were captured more efficiently at short times (Fig. 4A, black *versus* pink), although both reach high removal efficiencies (>80%) at 60 min (Fig. S48†). This result is consistent with the

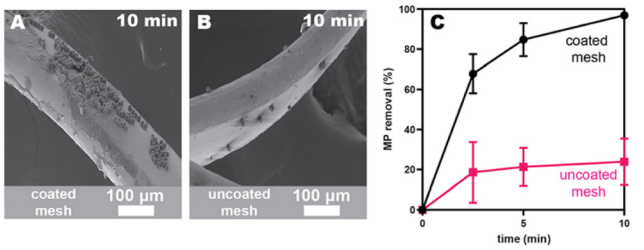

Fig. 2 SEM images of P_{EH} dip-coated stainless-steel mesh (A) and uncoated stainless-steel mesh (B) after 10 min of a capture experiment. (C) Plot of microplastic removal efficiencies (percent removed relative to a control) *versus* time (min), as quantified by flow cytometry. All capture experiments were performed in 80/20 water/ethanol solutions containing 500 mg L^{-1} of PS microplastics (10 μm diameter).

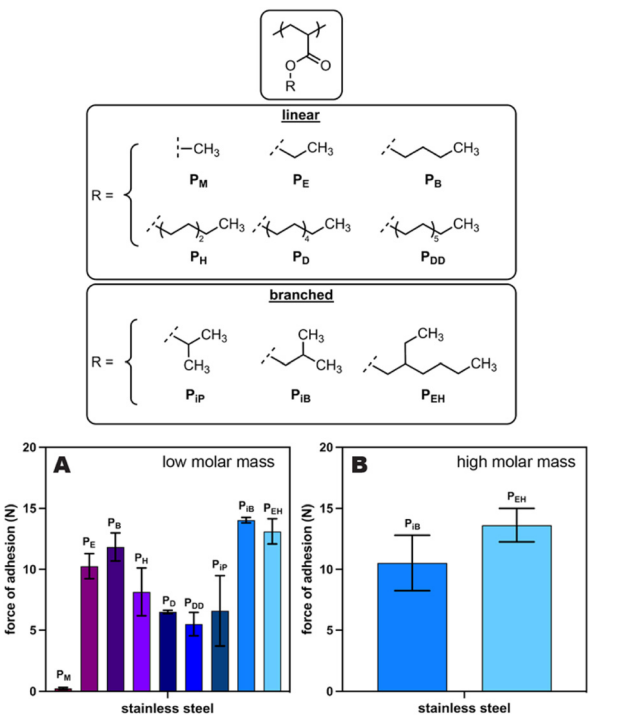

Fig. 3 (Top) Adhesive structures evaluated in probe-tack measurements. Plots of force of adhesion *versus* probe type using a stainless-steel probe for (A) low molar mass adhesives and (B) high molar mass adhesives.

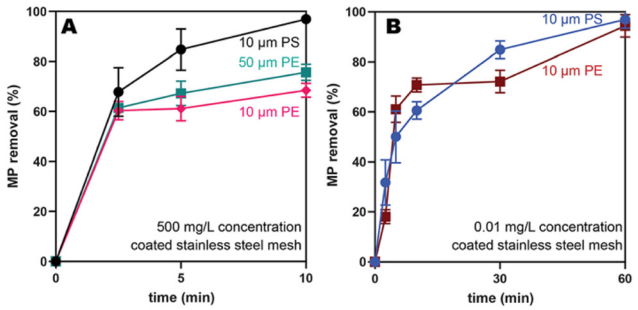

Fig. 4 Plots of microplastic removal efficiencies (percent removed relative to a control) *versus* time (min) for (A) PE (10 μm, 50 μm) and PS (10 μm) at a concentration of 500 mg L^{-1} in an 80/20 water/ethanol solution, and (B) PE (10 μm) and PS (10 μm) at a concentration of 0.01 mg L^{-1} in neat water. All experiments were performed using the adhesive-coated stainless-steel mesh.

probe-tack data, which showed that the PS exhibits a higher force of adhesion than PE to P_{EH} (14.4 N ± 1 *versus* 8.46 ± 0.5 N, Table S6†). Previous studies have shown that PS has more favorable van der Waals interactions with itself, compared to PE with itself, which would lead to aggregation and more efficient capture in water.[32]

To examine the impact of size, PE microplastics of varying sizes (10 *versus* 50 μm) were compared. The larger microplastics were captured more efficiently (75 ± 3% *versus* 68 ± 3% at 10 min, Fig. 4A, teal *versus* pink) albeit by a narrow margin. One explanation may be that the larger particles have more area available to facilitate wetting and ultimately capture by the adhesive. Combined, these results suggest that microplastic size and polymer identity only modestly impacts capture efficiencies.

Application to drinking water

To target concentrations like what is currently found in drinking water, PS and PE microplastics (10 μm) were compared at a significantly lower concentration (0.01 mg L^{-1}). Gratifyingly, both PS and PE exhibited high removal efficiencies at 60 min (97 ± 3% and 94 ± 5%, respectively; Fig. 4B) at these low concentrations. At shorter times (10 min), lower removal efficiencies (~60%; Fig. S50 and S51†) were observed. The slower capture at these lower concentrations is expected because there will be fewer collisions of the microplastics with the mesh. Interestingly, both PS and PE behave similarly at these low concentrations, in contrast to the slight preference for PS at higher concentrations. As a control, the uncoated stainless-steel mesh removed only 50% of both microplastics at 60 min (Fig. S50 and S51†), likely *via* nonspecific adsorption.

We also evaluated the capture efficiency for the larger microplastics (PE, 50 μm) at these low concentrations (0.01 mg L^{-1}). In this experiment, optical microscopy was utilized because there are so few particles (~140 microplastics per L). With this method, the microplastics can be counted after filtering a large volume of water through an aluminum oxide filter (200 nm pore size). To facilitate counting, brightly colored fluorescent pink PE microplastics (50 μm) were used. As a control, 100 mL of a microplastics stock solution was filtered to yield approximately 18 PE microplastics on the filter, close to the expected microplastics count (Table S13, and Fig. S52†). When this same stock solution was shaken with the P_{EH}-coated stainless-steel mesh, near quantitative (93%) removal of microplastics was observed (Table S13, and Fig. S53†). In contrast, the uncoated stainless-steel mesh removed only 50% of the PE microplastics, again *via* nonspecific adsorption (Table S13, and Fig. S54†). Combined, these results suggest that the adhesive-coated meshes are promising candidates for capturing microplastics at the small sizes and low concentrations observed in drinking water.

Conclusions and outlook

Herein, we demonstrated that adhesive-coated stainless-steel filters enhance the capture efficiency of pristine polystyrene and polyethylene microplastics at small (10 μm) and medium (50 μm) sizes, and under realistic contamination levels in drinking water (0.01 mg L^{-1}). Specifically, under realistic contamination levels, we observed >90% capture within 60 min. Combined, these results highlight how adsorption can be leveraged to supplement mechanical filtration. One advantage of this approach is that, after use, the adhesive coatings could be removed *via* solvent- or thermal-based methods, enabling one to potentially reuse or repurpose the microplastics, adhesive, and SS mesh. A life cycle assessment is needed to provide more insight into the potential scenarios, especially for the captured microplastics (*i.e.*, beyond landfilling or incineration). Future efforts should expand these studies to include other microplastic identities, sizes, and shapes, including environmental/weathered microplastics, as well as different water conditions.

Author contributions

The manuscript was written through contributions of all authors. MR, WJ, HET, and MEC were involved with conceptualization, data curation, formal analysis, investigation, methodology, validation, visualization, writing – reviewing and editing. SC was involved with investigation, methodology, and validation. AJM was involved with conceptualization, funding acquisition, project administration, resources, supervision, visualization, writing – original draft, review, and editing.

Conflicts of interest

There are no conflicts to declare.

Acknowledgements

The authors thank the National Science Foundation – Emerging Frontiers in Research and Innovation 2020 program for funding (#2029251).

References

1 Z. Luo, X. Zhou, Y. Su, H. Wang, R. Yu, S. Zhou, E. G. Xu and B. Xing, *Sci. Total Environ.*, 2021, **795**, 148902.
2 S. Yadav, N. Kataria, P. Khyalia, P. K. Rose, S. Mukherjee, H. Sabherwal, W. S. Chai, S. Rajendran, J.-J. Jiang and K. S. Khoo, *Chemosphere*, 2023, **326**, 138495.
3 J. Brahney, M. Hallerud, E. Heim, M. Hahnenberger and S. Sukumaran, *Science*, 2020, **368**, 1257–1260.
4 J. E. Bullard, A. Ockelford, P. O'Brien and C. McKenna Neuman, *Atmos. Environ.*, 2021, **245**, 118038.
5 E. K. Owowenu, C. F. Nnadozie, F. Akamagwuna, X. S. Noundou, J. E. Uku and O. N. Odume, *Aquat. Ecol.*, 2023, **57**, 557–570.
6 A. Portantino, SB-1263: Ocean Protection Council, *Statewide Microplastics Strategy*, 2018, **https://leginfo.legislature.ca.gov/faces/billTextClient.xhtml?bill_id=201720180SB1263**.
7 A. Portantino, SB-1422: California Safe Drinking Water Act: microplastics, 2018, **https://leginfo.legislature.ca.gov/faces/billTextClient.xhtml?bill_id=201720180SB1422**.
8 Q. Liu, Y. Chen, Z. Chen, F. Yang, Y. Xie and W. Yao, *Sci. Total Environ.*, 2022, **851**, 157991.
9 R. Ahmed, A. K. Hamid, S. A. Krebsbach, J. He and D. Wang, *Chemosphere*, 2022, **293**, 133557.
10 N. Badola, A. Bahuguna, Y. Sasson and J. S. Chauhan, *Front. Environ. Sci. Eng.*, 2022, **16**, 7.
11 S. L. Cherniak, H. Almuhtaram, M. J. McKie, L. Hermabessiere, C. Yuan, C. M. Rochman and R. C. Andrews, *Chemosphere*, 2022, **288**, 132587.
12 Y. Zhang, A. Diehl, A. Lewandowski, K. Gopalakrishnan and T. Baker, *Sci. Total Environ.*, 2020, **720**, 137383.
13 A. N. Velasco, S. R. Gentile, S. Zimmermann and S. Stoll, *Front. Water*, 2022, **4**, 835451.
14 A. S. Reddy and A. T. Nair, *Environ. Technol. Innov.*, 2022, **28**, 102815.
15 A. Sharma, S. Kumari, R. L. Chopade, P. P. Pandit, A. R. Rai, V. Nagar, G. Awasthi, A. Singh, K. K. Awasthi and M. S. Sankhla, *Sci. Prog.*, 2023, **106**, 00368504231176399.
16 L. Muthulakshmi, S. Mohan and T. Tatarchuk, *Environ. Sci. Pollut. Res.*, 2023, **30**, 84933–84948.
17 A. T. Adeleye, M. M. Bahar, M. Megharaj and M. M. Rahman, *J. Water Process Eng.*, 2023, **53**, 103777.
18 I. Ali, X. Tan, J. Li, C. Peng, P. Wan, I. Naz, Z. Duan and Y. Ruan, *Water Res.*, 2023, **230**, 119526.
19 Z. Chen, J. Fang, W. Wei, H. H. Ngo, W. Guo and B.-J. Ni, *J. Clean. Prod.*, 2022, **371**, 133676.
20 Y. Wang, M. Wang, Q. Wang, T. Wang, Z. Zhou, M. Mehling, T. Guo, H. Zou, X. Xiao, Y. He, X. Wang, O. J. Rojas and J. Guo, *Adv. Mater.*, 2023, **35**, 2301531.
21 T. T. V. Ha, N. M. Viet, P. T. Thanh and V. T. Quan, *Environ. Technol. Innov.*, 2023, **32**, 103265.
22 X. Rong, X. Chen, P. Li, C. Zhao, S. Peng, H. Ma and H. Qu, *Chemosphere*, 2022, **299**, 134493.
23 P. T. Chazovachii, J. M. Rieland, V. V. Sheffey, T. M. E. Jugovic, P. M. Zimmerman, O. Eniola-Adefeso, B. J. Love and A. J. McNeil, *ACS EST Engg.*, 2021, **1**, 1698–1704.
24 S. Mapari, S. Mestry and S. T. Mhaske, *Polym. Bull.*, 2021, **78**, 4075–4108.
25 D. Sol, C. Solís-Balbín, A. Laca, A. Laca and M. Díaz, *Sci. Total Environ.*, 2023, **899**, 165356.
26 P. T. Chazovachii, M. J. Somers, M. T. Robo, D. I. Collias, M. I. James, E. N. G. Marsh, P. M. Zimmerman, J. F. Alfaro and A. J. McNeil, *Nat. Commun.*, 2021, **12**, 4524.
27 Technibond Surface Energy Chart, **https://www.technibond.co.uk/wp-content/uploads/2019/04/surface-energy-chart.pdf** (accessed Oct 2023).
28 SUNHE 40 Pieces Lint Traps, For Washing Machine, **https://www.amazon.com/SUNHE-Pieces-Washing-Machine-Laundry/dp/B07594P4TV** (accessed Oct 2023).
29 A. Faghihnejad and H. Zeng, *Soft Matter*, 2012, **8**, 2746–2759.
30 T. Jugovic, M. Robo, W. Ji, M. E. Clough, A. J. McNeil and P. Zimmerman, submitted.
31 J. M. Rieland, Z. Hu, J. S. Deese and B. J. Love, *Sep. Purif. Technol.*, 2023, **307**, 122819.
32 C.-Q. Wang, H. Wang, G.-H. Gu, J.-G. Fu, Q.-Q. Lin and Y.-N. Liu, *Waste Manage.*, 2015, **46**, 56–61.